Contents lists available at ScienceDirect

Review of Palaeobotany and Palynology

Shedding light on sporopollenin chemistry, with reference to UV reconstructions

Phillip E. Jardine [a,*], Feargus A.J. Abernethy [b], Barry H. Lomax [c], William D. Gosling [a,d], Wesley T. Fraser [a,e]

[a] *School of Environment, Earth and Ecosystem Sciences, The Open University, Walton Hall, Milton Keynes, MK7 6AA, UK*
[b] *School of Physical Sciences, The Open University, Walton Hall, Milton Keynes, MK7 6AA, UK*
[c] *Agriculture and Environmental Science, University of Nottingham, Sutton Bonington Campus, Leicestershire, LE12 5RD, UK*
[d] *Palaeoecology & Landscape Ecology, Institute of Biodiversity & Ecosystem Dynamics (IBED), University of Amsterdam, 1090 GE Amsterdam, The Netherlands*
[e] *Geography, Department of Social Sciences, Oxford Brookes University, Oxford OX3 0BP, UK*

ABSTRACT

Sporopollenin, which forms the outer wall of pollen and spores, contains a chemical signature of ultraviolet-B flux via concentrations of UV-B absorbing compounds (UACs), providing a proxy for reconstructing UV irradiance through time. Although Fourier transform infrared (FTIR) spectroscopy provides an efficient means of measuring UAC concentrations, nitrogen-containing compounds have the potential to bias the aromatic and hydroxyl bands used to quantify and standardise UAC abundances. Here, we explore the presence and possible influence of nitrogen in UV reconstruction via an FTIR study of *Lycopodium* spores from a natural shading gradient. We show that the UV-sensitive aromatic peak at 1510 cm^{-1} is clearly distinguishable from the amide II peak at 1550 cm^{-1}, and the decrease in aromatic content with increased shading can be reconstructed using standardisation approaches that do not rely on the 3300 cm^{-1} hydroxyl band. Isolation of the sporopollenin results in the loss of nitrogen-related peaks from the FTIR spectra, while the aromatic gradient remains. This confirms the lack of nitrogen in sporopollenin and its limited potential for impacting on palaeo-UV reconstructions. FTIR is therefore an appropriate tool for quantifying UACs in spores and pollen, and information on UV flux should be obtainable from fossil or processed samples.

© 2016 The Authors. Published by Elsevier B.V. This is an open access article under the CC BY license (http://creativecommons.org/licenses/by/4.0/).

1. Introduction

Pollen and spores (collectively sporomorphs), the reproductive vectors of land plants, contain a chemical signature of prevailing ultraviolet-B flux that can be used as a proxy for reconstructing UV-B through time (Rozema et al., 2009; Fraser et al., 2014a). Plant tissues contain UV-B absorbing compounds (UACs), a natural sun block that protects the cellular machinery from the harmful effects of UV-B (Rozema et al., 2009; Lomax and Fraser, 2015). Critically, plants have the ability to upregulate UAC production in response to increases in UV-B exposure, providing the basis for a UV-B proxy (Rozema et al., 1997; Rozema et al., 1999; Rozema et al., 2001a; Rozema et al., 2001b; Lomax et al., 2008; Rozema et al., 2009). In sporomorphs UV absorption occurs primarily in the outer wall or exine (Rozema et al., 2009), which is composed of sporopollenin, a biopolymer that is highly resistant to chemical, biological and physical attack (Brooks and Shaw, 1968, 1978; Mackenzie et al., 2015), providing plants with a fossil record that extends to the Ordovician, ~470 million years ago (Rubenstein et al., 2010). The UACs in sporopollenin are the phenolic compounds *p*-

coumaric acid and ferulic acid, which form cross-links between straight chain aliphatic compounds (the other major component of sporopollenin), and absorb solar UV-B through their aromatic ring structure (Blokker et al., 2005; Rozema et al., 2009). Measurable increases in the concentrations of UACs in sporopollenin in response to enhanced UV flux have been documented in a variety of settings (Watson et al., 2007; Lomax et al., 2008; Fraser et al., 2011; Willis et al., 2011; Lomax et al., 2012), opening up the possibility of reconstructing UV-B and its covariates (e.g. solar irradiance, ozone thickness [Rozema, 2002; Lomax et al., 2008], altitude [Lomax et al., 2012]) through geological time.

Initial insights into sporopollenin chemistry and UAC measurement were carried out using pyrolysis GC–MS and thermochemolysis-GC–MS (Blokker et al., 2005; Watson et al., 2007; Watson et al., 2012). GC–MS-based analyses are however relatively costly, time consuming, and destructive. Fourier transform infrared (FTIR) spectroscopy provides an alternative means of measuring UAC concentrations, via the aromatic (C=C) peak that occurs between 1510 and 1520 cm^{-1} (Watson et al., 2007; Lomax et al., 2008; Fraser et al., 2011; Lomax et al., 2012; Jardine et al., 2015). Since the absolute peak height relates to sample thickness as well as UAC concentrations, this peak has previously been normalised against the broad hydroxyl (OH) absorbance band at

~3300 cm^{-1}, since this is internally stable in FTIR sporopollenin spectra (Watson et al., 2007; Lomax et al., 2008).

FTIR provides an efficient, economic, and non-destructive means of accumulating large data sets to assess sporomorph chemistry, enabling proxy development. However, there are possible confounding factors in measuring UAC concentrations from FTIR spectra. In particular, the presence of nitrogen-containing compounds may bias measurement of the 1510 cm^{-1} aromatic peak (Rozema et al., 2009). Nitrogen is known to occur in proteins in sporomorphs, and occurs in vibrational spectra through amide groups that represent the protein backbone, and other bonds that relate to specific amino acid side-chains (Barth and Zscherp, 2002; Schulte et al., 2008).

Of particular relevance is the position of the amide II band in sporomorph vibrational spectra. This band results primarily from the out-of-phase combination of NH bending and CN stretching (Barth and Zscherp, 2002; Miller, 2003), and typically occurs at ~1550 cm^{-1} but can also be present at sufficiently low wavenumbers (Miller, 2003) to be conflated with, or impact upon, the 1510 cm^{-1} aromatic peak. The amino acid tyrosine, which has previously been identified in pollen grains (Schulte et al., 2008), also occurs as an aromatic peak at ~1517 cm^{-1} (Barth and Zscherp, 2002), within the frequency range of the UAC peak. The height of the 3300 cm^{-1} hydroxyl band that is used to normalise the 1510 cm^{-1} aromatic peak may also be influenced by amide groups, either from the amide A and B bands, which represent NH stretching and occur at ~3300 and 3170 cm^{-1} (Barth and Zscherp, 2002; Miller, 2003; Rozema et al., 2009), respectively, or through overtones of the amide II band (Miller, 2003). It has been suggested (Rozema et al., 2009) that the aromatic/hydroxyl ratio may relate partly to sporopollenin macromolecular structure, rather than UAC concentrations.

Critical to understanding the influence of nitrogen on UAC quantification is the location of nitrogen-containing compounds within sporomorphs. Proteins are known to occur in the cytoplasm and in compounds external to the sporomorph wall (Traverse, 2007; Pummer et al., 2012; Pummer et al., 2013), but GC–MS analysis of sporopollenin itself has not yielded nitrogen-containing compounds (Watson et al., 2007; Mackenzie et al., 2015). If this is the case the influence of nitrogen on FTIR spectra should be limited when applied to fossil or processed sporomorphs where only the sporopollenin component remains. However, the impact of nitrogen has not been explicitly studied across a UV-B gradient, and this and other potential confounding effects need to be understood for the successful analysis of both modern (experimental and herbarium) and fossil samples.

Here, we address these issues by re-analysing the FTIR dataset of Fraser et al. (2011), which documents statistically significant changes in the UAC concentrations of *Lycopodium annotinum* Linnaeus spores across a natural shading gradient. Specifically, we:

1. Attempt to identify both amide and UAC peaks in the FTIR spectra.

2. Study changes in the 1510 cm^{-1} aromatic peak height across the shading gradient, from spectra that have been standardised to zero mean and unit variance (i.e. z-scores; Jardine et al., 2015). This standardisation approach removes the effect of sample thickness on the peak heights, and so does not rely on normalising against the 3300 cm^{-1} hydroxyl band. This allows us to determine whether the previously reconstructed UAC gradient (Fraser et al., 2011) is still present without the influence of the hydroxyl band.

3. Compare the spectra of untreated and acetolysed spores. Acetolysis is an oxidation technique that efficiently removes all of the non-sporopollenin components of sporomorphs, including the cytoplasm, inner wall, and outer proteins and lipids (Traverse, 2007; Jardine et al., 2015). This allows us to determine whether the amide peaks remain following acetolysis and therefore the likely influence of nitrogen-containing compounds on UAC measurement in fossil or processed sporomorphs.

2. Materials and methods

The published FTIR dataset of Fraser et al. (2011) comprises samples of *Lycopodium annotinum* spores from Abisko, Sweden (68° 21′ N, 18° 49′ E). The samples were collected in September 2006 from six plants: three in the full shade of the tree canopy (samples E10-6A, E10-6B and E10-6C), two in partial shade at the forest margin (samples E10-5A and E10-5B), and one under open sky (sample E10-7B). The Fraser et al. (2011) dataset comprises five replicate FTIR spectra from each sample, except for sample E10-6A where four replicates were analysed. We have used the same samples to carry out FTIR analysis of acetolysed spores.

The spore exine was isolated by acetolysing the samples for 10 min at 90 °C in a water bath, using a standard preparation of nine parts acetic anhydride ([CH$_3$CO]$_2$O) to one part sulfuric acid (H$_2$SO$_4$) (Faegri and Iversen, 1989). After 10 min the centrifuge tubes were topped up with glacial acetic acid (CH$_3$COOH) to stop the reaction, centrifuged and the supernatant decanted. The centrifuge tubes were then topped up with water, centrifuged and decanted a further three times.

FTIR analysis of the acetolysed spores was carried out using the same equipment and protocol as in the original study (Fraser et al., 2011). Specifically, we used a Thermo Scientific (Waltham, MA, USA) Nicolet Nexus FTIR bench unit with a Continuum IR microscope fitted with a MCT-A liquid nitrogen-cooled detector in transmission mode using a Reflachromat 15× objective lens. To remove atmospheric H$_2$O and CO$_2$ interference within spectra the entire system (bench unit, microscope and sample stage) was purged with air that has been dried and scrubbed of CO$_2$ using a Peak Scientific (Billerica, MA, USA) ML85 purge unit. We collected five replicate scans for each sample, using an aperture size of 100 × 100 μm at 512 scans per replicate and a resolution of 1.928 cm^{-1} wavenumbers. A background scan was taken before each analytical run and automatically subtracted from the sample spectrum.

All data manipulation and analysis was carried out in R version 3.2.1 (R Development Core Team, 2015). Baseline drift was corrected for by subtracting a linear baseline from each sample. Baseline removal was carried out using the R package 'baseline' 1.2–0 (Liland and Mevik, 2015) with the 'modpolyfit' method, which fits the baselines by least squares polynomial curve fitting, in this case with a first-order polynomial baseline (Lieber and Mahadevan-Jansen, 2003). Following baseline correction, each spectrum was standardised to zero mean and unit variance (z-scores) using the equation $(x - \bar{x}) / \sigma$, where x is the absorbance value, $\bar{x}$ is the spectrum arithmetic mean, and σ is the spectrum standard deviation.

For each standardised FTIR spectrum the heights of the 1510 cm^{-1} aromatic peak and the 3300 cm^{-1} hydroxyl peak were measured. Peak heights were measured by taking the maximum value within a given range, which was 1505 to 1525 cm^{-1} for the aromatic peak, and 3190 to 3550 cm^{-1} for the hydroxyl peak. For comparison with the standardised peak heights both peaks were also measured in the baseline corrected, unstandardised spectra, and the aromatic/OH ratio calculated. The statistical significance of differences in peak heights among the three shading levels was assessed with non-parametric Kruskal-Wallace tests (Hammer and Harper, 2006). Other bands were assigned to functional groups and sporomorph components (i.e., sporopollenin, proteins, lipids) using the literature (Coates, 2000; Mayo, 2003; Watson et al., 2007; Schulte et al., 2008; Schulte et al., 2010; Zimmermann, 2010; Fraser et al., 2011; Larkin, 2011; Fraser et al., 2012; Pummer et al., 2013; Fraser et al., 2014b; Zimmermann and Kohler, 2014; Bağcıoğlu et al., 2015; Zimmermann et al., 2015a; Zimmermann et al., 2015b); those discussed in this paper are summarized in Table 1. All raw spectral data and R code used for data analysis are included in the Supplementary Information.

Table 1

Band assignments for absorbance bands discussed in the text. Interpretation follows the literature (Coates, 2000; Mayo, 2003; Watson et al., 2007; Schulte et al., 2008; Schulte et al., 2010; Zimmermann, 2010; Fraser et al., 2011; Larkin, 2011; Fraser et al., 2012; Pummer et al., 2013; Fraser et al., 2014b; Zimmermann and Kohler, 2014; Bağcıoğlu et al., 2015; Zimmermann et al., 2015a; Zimmermann et al., 2015b). δ = bending, v = stretching, s = symmetrical, as = asymmetrical.

Wavenumber (cm^{-1})	Band assignment	Interpretation
3300	vOH	Hydroxyl
2925	vasCHn	Aliphatic, lipids and sporopollenin
2850	vsCHn	Aliphatic, lipids and sporopollenin
1740	vC = O	Lipids
1710	vC = O	Carboxyl, sporopollenin
1650	vC = O	Amide I, proteins
1600	vC = C	Aromatic, sporopollenin
1550	δNH, vC-N	Amide II, proteins
1510	vC = C	Aromatic, sporopollenin
1460	δCH$_2$	Aliphatic, lipids
1440	δ_C-H	Aromatic, proteins and sporopollenin
1265	δNH, vC-N	Amide III, proteins
1160	vC-H	Aromatic, sporopollenin
1030	vC-H	Aromatic, sporopollenin
853	δ_C-H	Aromatic, proteins and sporopollenin
817	δ_C-H	Aromatic, sporopollenin

3. Results

Analysis of FTIR spectra from untreated *Lycopodium* spores shows that both amide and aromatic peaks are present and identifiable (Fig. 1A and B). The amide I peak, which relates to C=O stretching and occurs at ~1650 cm^{-1} (Barth and Zscherp, 2002; Miller, 2003; Schulte et al., 2008) is more prominent than the amide II peak at 1550 cm^{-1}. The amide III peak, which is the in-phase combination of NH bending and CN stretching (Barth and Zscherp, 2002; Miller, 2003), has previously been identified in Raman spectra at ~1270 cm^{-1} (Schulte et al., 2008) but is not strongly expressed in FTIR (Miller, 2003) and is not identifiable in the *Lycopodium* spectra. The aromatic peak at 1510 cm^{-1} is clearly detectable, and importantly this peak and the amide II peak are distinguishable from each other.

A number of other peaks identified in previous studies (Watson et al., 2007; Schulte et al., 2008; Schulte et al., 2010; Zimmermann, 2010; Fraser et al., 2011; Fraser et al., 2012; Pummer et al., 2013; Fraser et al., 2014b; Bağcıoğlu et al., 2015; Zimmermann et al., 2015a) can be identified in the *Lycopodium* spectra (Fig. 1A and B, Table 1). Peaks relating to C=C or C—H bonds in aromatic ring structures (Coates, 2000) are present at 1160 cm^{-1}, 853 cm^{-1}, and 817 cm^{-1}, in addition to the aromatic peak at 1510 cm^{-1}. A carbonyl (C = O) band at 1740 cm^{-1} and an aliphatic (CH$_2$) band at 1460 cm^{-1} represent lipids (Bağcıoğlu et al., 2015). Prominent vasCH$_n$ and vsCH$_n$ aliphatic peaks also occur at 2925 and 2850 cm^{-1}, respectively. Carbohydrates occur as small peaks in the 1200 to 900 cm^{-1} range (Bağcıoğlu et al., 2015).

The distributions of peak height measurements within samples are shown as box plots (Fig. 2) while the shading treatment medians are displayed in bar charts (Fig. 3). Peak heights from the standardised spectra show that the 1510 cm^{-1} aromatic peak (Figs. 2A and 3A) responds as expected across the shading gradient, with a statistically significant ($H = 6.62, df = 2, p = 0.037$) decrease in height with increased shading, consistent with earlier findings (Fraser et al., 2011). The hydroxyl peak shows no clear relationship with shading level (Figs. 2C and 3C; $H = 1.49, df = 2, p = 0.48$). Standardising the aromatic peak by the hydroxyl peak (Figs. 2E and 3E) shows the same overall relationship as the z-score standardised peak height (Figs. 2A and 3A), with a significant decrease in peak height ratio across the shading gradient ($H = 10.23, df = 2, p = 0.006$).
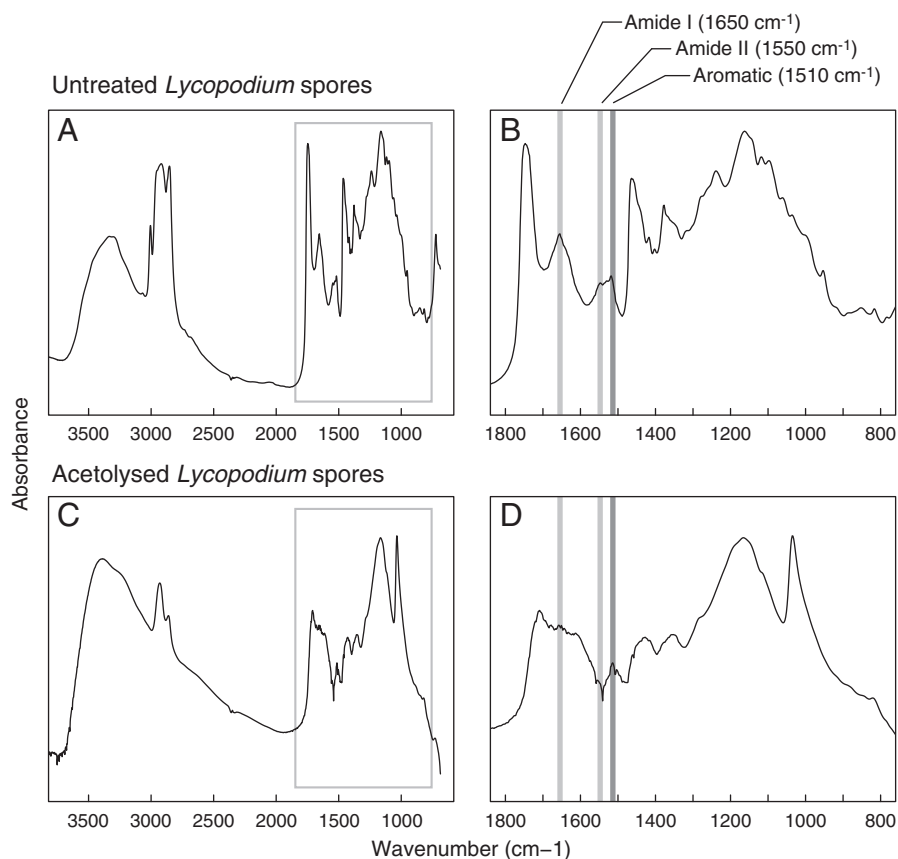

Fig. 1. *Z*-score standardised FTIR mean spectra of unprocessed (A and B) and acetolysed (C and D) *Lycopodium* spores. A and C show the full spectra, and B and D show the 1800 to 800 cm^{-1} range, with the positions of the amide I and II peaks and the 1510 cm^{-1} aromatic peak highlighted.
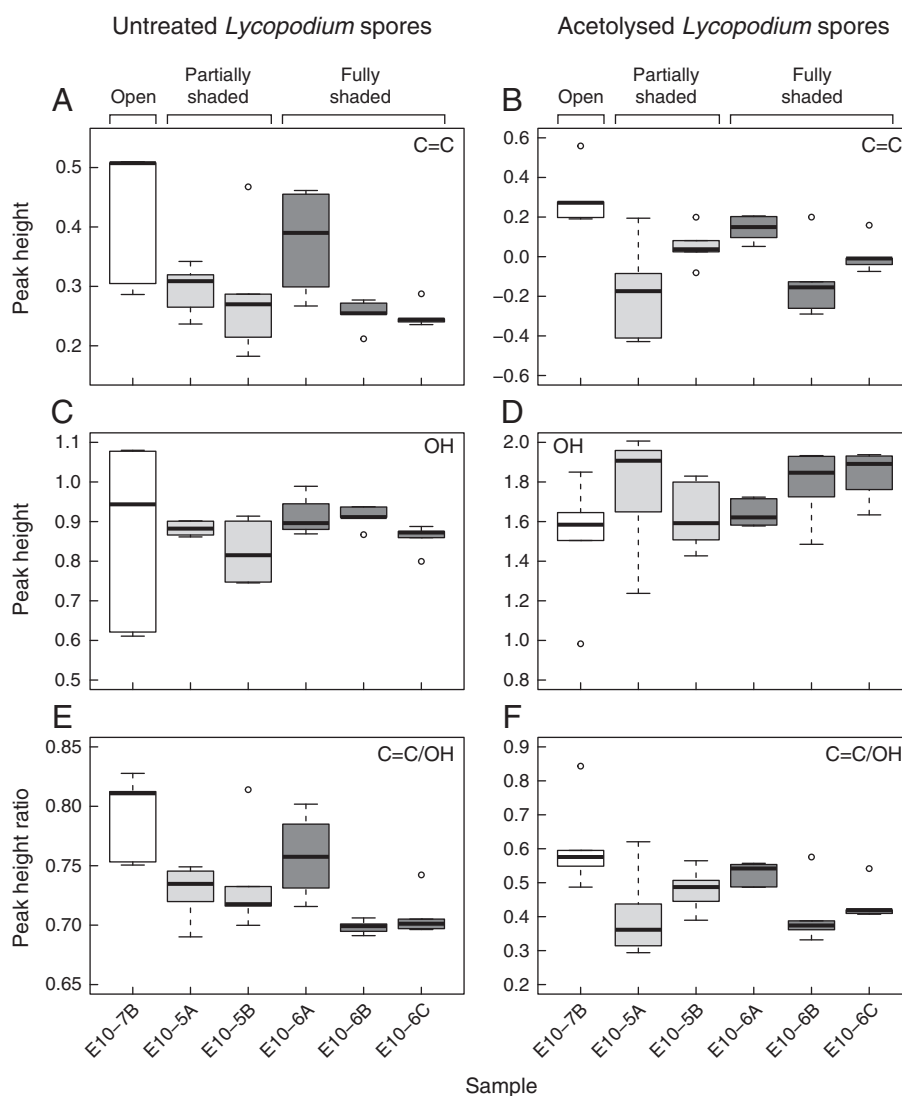
Fig. 2. Boxplots of FTIR peak height changes across the shading gradient, for unprocessed (A, C, and E) and acetolysed (B, D, and F) *Lycopodium* spores. A and B show the z-score standardised 1510 cm^{-1} aromatic peak, C and D the z-score standardised 3300 cm^{-1} hydroxyl peak, and E and F the aromatic/hydroxyl ratio from the unstandardised spectra. Box colours relate to the level of shading: white = open (unshaded) sample, light grey = partially shaded samples, dark grey = fully shaded samples. For each sample the thick horizontal line equals the median value, the edges of the box the lower and upper quartiles, the whiskers show the extremes of the data up to 1.5 times the interquartile range, and individual data points show any outliers beyond this.

Acetolysis leads to a simplification of the FTIR spectra, with a number of peaks reducing in size or disappearing altogether (Fig. 1C and D). While the 1510 cm^{-1} aromatic peak remains distinct the amide I and II peaks are reduced in height, to the extent that they almost completely disappear from the spectrum. Acetolysis also reduces or removes other peaks relating to lipids, carbohydrates, and aromatic compounds (Fig. 1C and D). The vasCH$_n$ and vsCH$_n$ aliphatic peaks at 2925 and 2850 cm^{-1} are reduced in height, the 1460 cm^{-1} peak almost disappears, but a broad absorbance band remains at 1440 cm^{-1}. The 1740 cm^{-1} carbonyl peak disappears, and the small carbohydrate peaks in the 1200 to 900 cm^{-1} region are also removed. The aromatic peak at 850 cm^{-1} disappears, and an aromatic peak at 1600 cm^{-1} (Fraser et al., 2014b; Jardine et al., 2015) emerges. A carboxyl peak at 1710 cm^{-1} also emerges following acetolysis, as does a prominent peak at 1030 cm^{-1} which is only weakly apparent in the fresh material, and probably represents ferulic acid (Bağcıoğlu et al., 2015). The peaks at 1370 and 1160 cm^{-1} remain in a simplified form. The

shape of the hydroxyl absorbance band at ~3300 cm^{-1} also changes, with the main peak shifting to higher wavenumbers.

Box plots and bar charts of peak heights for the acetolysed spores show that the aromatic gradient is still present after acetolysis (Figs. 2B and 3B), with a significant difference in median peak height among the shading levels ($H = 9.46$, $df = 2$, $p = 0.009$). The hydroxyl peak (Figs. 2D and 3D) shows slightly more variability compared to the fresh material (Figs. 2C and 3C), but the range of values is still similar across the shading gradient and the difference in peak height is not statistically significant ($H = 2.52$, $df = 2$, $p = 0.28$). Standardising the aromatic peak by the hydroxyl peak (Figs. 2F and 3F) leads to a similar reconstruction to the z-score standardised aromatic peak (Figs. 2B and 3B), and the difference among shading levels is again significant ($H = 6.44$, $df = 2$, $p = 0.04$). Importantly, the overall magnitude of the aromatic peak height decrease from the open to partially and fully shaded samples is similar in the fresh and acetolysed material (~0.25 standard deviations in the z-score standardised spectra, and ~0.1 in terms of the aromatic/hydroxyl ratio [Fig. 3]).
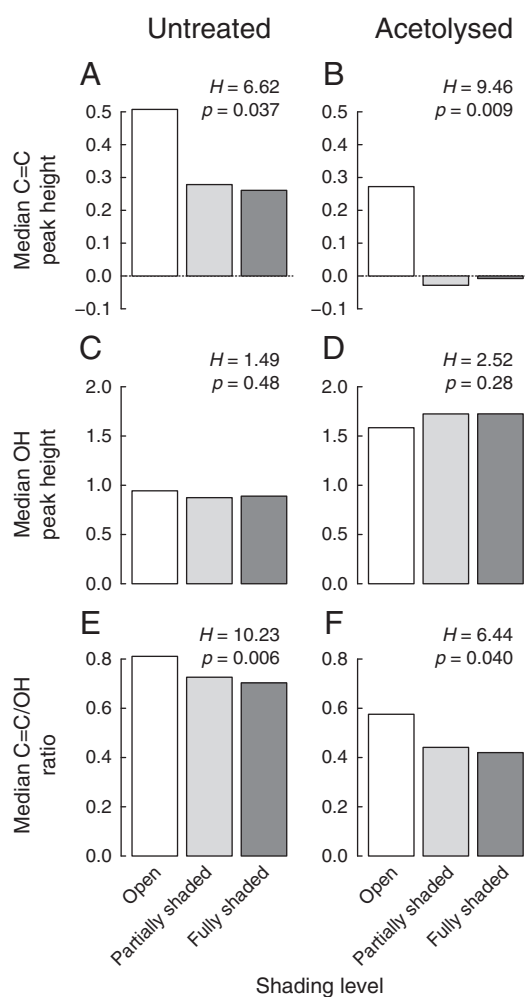
Fig. 3. Barcharts of shading treatment median peak heights, for unprocessed (A, C, and E) and acetolysed (B, D, and F) *Lycopodium* spores. A and B show the z-score standardised 1510 cm^{-1} aromatic peak, C and D the z-score standardised 3300 cm^{-1} hydroxyl peak, and E and F the aromatic/hydroxyl ratio from the unstandardised spectra. Bar colours relate to the level of shading: white = open (unshaded) sample, light grey = partially shaded samples, dark grey = fully shaded samples. *H* and *p* values are the results of Kruskal-Wallace tests of equality among shading level peak height medians.

4. Discussion

The results of this study are consistent with previous research (Zimmermann and Kohler, 2014; Bağcıoğlu et al., 2015; Zimmermann et al., 2015a) that has identified amide and aromatic peaks in sporomorph FTIR spectra. Amide I and II peaks, and the aromatic peak at 1510 cm^{-1} that is the basis of the UV-B proxy (Watson et al., 2007; Fraser et al., 2014a), are clearly and consistently distinguishable in such diverse taxa as *Lycopodium* (this study), gymnosperms of the Pinaceae and Podocarpaceae families (Bağcıoğlu et al., 2015), and angiosperms of the Liliaceae, Oleaceae and Plantaginaceae families (Zimmermann and Kohler, 2014). This demonstrates that the 1510 cm^{-1} aromatic peak provides an indicator of sporopollenin UAC concentrations that is independent of the influence of the amide II peak.

The height of the 3300 cm^{-1} hydroxyl peak does not show any statistically significant trend across the shading gradient (Fig. 3). Similar patterns in the height of the 1510 cm^{-1} aromatic peak are reconstructed when normalising by the hydroxyl peak or using z-score standardisation, which demonstrates that the height of the hydroxyl peak is robust to nitrogen-containing compounds absorbing in the same part of the spectrum. The shape of the hydroxyl absorbance band does change following acetolysis (Fig. 1), possibly as a result of

the loss of proteins or hydroxyl groups occurring outside of the sporopollenin. However, the recovery of a similar, statistically significant trend in aromatic peak height in the acetolysed spores suggests that this is not problematic for the UV-B proxy, and that standardising by the hydroxyl band or z-scores should give accurate results.

The removal or reduction of the amide peaks following acetolysis, along with peaks relating to lipids, carbohydrates and other protein bonds, is consistent with these compounds occurring outside of the sporopollenin component of spores and pollen (Pummer et al., 2012; Pummer et al., 2013; Jardine et al., 2015). Any environmentally driven trends in these compounds (Zimmermann and Kohler, 2014) will therefore not be detected in fossil samples where only the sporopollenin is preserved, regardless of their peak positions in relation to the UV-sensitive aromatic peaks. This is especially important in the case of the tyrosine peak, which occurs at 1517 cm^{-1} (Barth and Zscherp, 2002) and therefore cannot be separated out as easily as the amide II band. The previously documented reduction in the height of the 1510 cm^{-1} peak with acetolysis (Jardine et al., 2015) may relate to the loss of this amino acid from sporomorphs.

Importantly, these results show for the first time that a recoverable response to UV-B flux is present in isolated sporopollenin, and is measurable in FTIR. This supports the expectation (Fraser et al., 2014a) that sporopollenin preserved in the fossil record should contain a sufficient signature of the UV-B response to be detected using FTIR as an analytical tool.

Recent research has shown the potential of using isolated sporomorph exines as microparticles and microcapsules, with a rapidly growing array of uses in material science, food, and pharmaceutical applications (Mackenzie et al., 2015). A full understanding of sporopollenin chemistry, and the impact of other substances on it, is essential for these activities, and FTIR provides a rapid method for assessing this. Our results highlight the importance of using the spectra of acetolysed (or otherwise processed) spores and pollen when evaluating sporopollenin chemistry, rather than the spectra of fresh grains. This is important first because strong peaks in the acetolysed spectra, such as the peak at 1030 cm^{-1} (Fig. 1), can be obscured in the fresh spectra. Second, and as already noted, some aromatic and aliphatic peaks relate in part to the labile components outside of the sporopollenin (Pummer et al., 2012; Pummer et al., 2013; Jardine et al., 2015), and are reduced in height when the sporopollenin is isolated. In the current study this is observed in the aromatic peak at 850 cm^{-1} and the aliphatic peaks at 2925 and 2850 cm^{-1}, which are reduced with acetolysis. In these cases it is likely that the peaks relate to compounds that occur both within the sporopollenin and external to it, and it is only with the spectra of isolated exines that accurate estimates of sporopollenin chemistry can be derived.

5. Conclusion

We have shown that the presence of nitrogen in the proteins of sporomorphs does not hinder the measurement of UAC concentrations using FTIR. The amide groups are clearly distinct from the UV-B responsive 1510 cm^{-1} aromatic peak, do not alter the height of the hydroxyl band that has been used to normalise the aromatic peak, and are entirely or mostly limited to compounds occurring external to the sporopollenin, and so are of little relevance to studies of fossil sporomorphs. We have also demonstrated that the same phenolic gradient that is present in fresh (i.e., unprocessed) spores is recoverable from isolated sporopollenin. Given the high preservation potential of sporopollenin in the fossil record, we anticipate that UV reconstructions are fully achievable even in deep time settings.

Appendix A. Supplementary data

Supplementary data to this article can be found online at http://dx.doi.org/10.1016/j.revpalbo.2016.11.014.

References

Bağcıoğlu, M., Zimmermann, B., Kohler, A., 2015. A multiscale vibrational spectroscopic approach for identification and biochemical characterization of pollen. PLoS One 10, 1–19.

Barth, A., Zscherp, C., 2002. What vibrations tell about proteins. Q. Rev. Biophys. 35, 369–430.

Blokker, P., Yeloff, D., Boelen, P., Broekman, R.A., Rozema, J., 2005. Development of a proxy for past surface UV-B irradiation: a thermally assisted hydrolysis and methylation py-GC/MS method for the analysis of pollen and spores. Anal. Chem. 77, 6026–6031.

Brooks, J., Shaw, G., 1968. Chemical structure of the exine of pollen walls and a new function for carotenoids in nature. Nature 219, 532–533.

Brooks, J., Shaw, G., 1978. Sporopollenin: a review of its chemistry, palaeochemistry and geochemistry. Grana 17, 91–97.

Coates, J., 2000. Interpretation of infrared spectra, a practical approach. In: Meyers, R.A. (Ed.), Encyclopedia of Analytical Chemistry. John Wiley and Sons Ltd., Chichester, pp. 10815–10837.

Development Core Team, R., 2015. R: A Language and Environment for Statistical Computing. R Foundation for Statistical Computing, Vienna, Austria (http://www.R-project.org/).

Faegri, K., Iversen, J., 1989. Textbook of Pollen Analysis. fourth ed. John Wiley & Sons, New York.

Fraser, W.T., Sephton, M.A., Watson, J.S., Self, S., Lomax, B.H., James, D.I., Wellman, C.H., Callaghan, T.V., Beerling, D.J., 2011. UV-B absorbing pigments in spores: biochemical responses to shade in a high-latitude birch forest and implications for sporopollenin-based proxies of past environmental change. Polar Res. 30:8312. http://dx.doi.org/10.3402/polar.v30i0.8312.

Fraser, W.T., Scott, A.C., Forbes, A.E.S., Glasspool, I.J., Plotnick, R.E., Kenig, F., Lomax, B.H., 2012. Evolutionary stasis of sporopollenin biochemistry revealed by unaltered Pennsylvanian spores. New Phytol. 196, 397–401.

Fraser, W.T., Lomax, B.H., Jardine, P.E., Gosling, W.D., Sephton, M.A., 2014a. Pollen and spores as a passive monitor of ultraviolet radiation. Front. Ecol. Evol. 2:12. http://dx.doi.org/10.3389/fevo.2014.00012.

Fraser, W.T., Watson, J.S., Sephton, M.A., Lomax, B.H., Harrington, G., Gosling, W.D., Self, S., 2014b. Changes in spore chemistry and appearance with increasing maturity. Rev. Palaeobot. Palynol. 201, 41–46.

Hammer, Ø., Harper, D.A.T., 2006. Paleontological Data Analysis. Blackwell Publishing, Oxford.

Jardine, P.E., Fraser, W.T., Lomax, B.H., Gosling, W.D., 2015. The impact of oxidation on spore and pollen chemistry. J. Micropalaeontol. 34, 139–149.

Larkin, P.J., 2011. Infrared and Raman Spectroscopy: Principals and Spectral Interpretation. Elsevier, Waltham, MA, USA.

Lieber, C.A., Mahadevan-Jansen, A., 2003. Automated method for subtraction of fluorescence from biological Raman spectra. Appl. Spectrosc. 57, 1363–1367.

Liland, K.H., Mevik, B.-H., 2015. Baseline, R Package Version 1.2–0.

Lomax, B.H., Fraser, W.T., 2015. Palaeoproxies: botanical monitors and recorders of atmospheric change. Palaeontology 58, 759–768.

Lomax, B.H., Fraser, W.T., Sephton, M.A., Callaghan, T.V., Self, S., Harfoot, M., Pyle, J.A., Wellman, C.H., Beerling, D.J., 2008. Plant spore walls as a record of long-term changes in ultraviolet-B radiation. Nat. Geosci. 1, 592–596.

Lomax, B.H., Fraser, W.T., Harrington, G., Blackmore, S., Sephton, M.A., Harris, N.B.W., 2012. A novel palaeoaltimetry proxy based on spore and pollen wall chemistry. Earth Planet. Sci. Lett. 353-354, 22–28.

Mackenzie, G., Boa, A.N., Diego-Taboada, A., Atkin, S.L., Sathyapalan, T., 2015. Sporopollenin, the least known yet toughest natural biopolymer. Front. Mater. 2, 1–5.

Mayo, D.W., 2003. Survey of infrared and Raman group frequencies. In: Mayo, D.W., Miller, F.A., Hannah, R.W. (Eds.), Course Notes on the Interpretation of Infrared and Raman Spectra. John Wiley and Sons, Inc., New Jersey, pp. 355–398.

Miller, F.A., 2003. Amides, carboxylate ion, and C—O single bonds. In: Mayo, D.W., Miller, F.A., Hannah, R.W. (Eds.), Course Notes on the Interpretation of Infrared and Raman Spectra. John Wiley and Sons, New Jersey, pp. 205–216.

Pummer, B.G., Bauer, H., Bernardi, J., Bleicher, S., Grothe, H., 2012. Suspendable macromolecules are responsible for ice nucleation activity of birch and conifer pollen. Atmos. Chem. Phys. 12, 2541–2550.

Pummer, B.G., Bauer, H., Bernardi, J., Chazallon, B., Facq, S., Lendl, B., Whitmore, K., Grothe, H., 2013. Chemistry and morphology of dried-up pollen suspension residues. J. Raman Spectrosc. 44, 1654–1658.

Rozema, J., 2002. Toward solving the UV puzzle. Science 296, 1621–1622.

Rozema, J., van de Staij, J., Björn, L.-O., Caldwell, M., 1997. UV-B as an environmental factor in plant life: stress and regulation. Trends Ecol. Evol. 12, 22–28.

Rozema, J., van de Staaij, J., Björn, L.-O., de Bakker, N., 1999. Depletion of stratospheric ozone and solar UV-B radiation: Evolution of land plants, UV-screens and functions of polyphenolics. In: Rozema, J. (Ed.), Stratospheric Ozone Depletion: The Effects of Enhanced UV-B Radiation on Terrestrial Ecosystems. Backhuys, Leiden, pp. 1–19.

Rozema, J., Broekman, R.A., Blokker, P., Meijkamp, B., de Bakker, N., van de Staaij, J., van Beem, A., Ariese, F., Kars, S.M., 2001a. UV-B absorbance and UV-B absorbing compounds (para-coumaric acid) in pollen and sporopollenin: the perspective to track historic UV-B levels. J. Photochem. Photobiol. B Biol. 62, 108–117.

Rozema, J., Noordjik, A.J., Broekman, R.A., van Beem, A., Meijkamp, B.M., de Bakker, N.V.J., van de Staaij, J.W.M., Stroetenga, M., Bohncke, S.J.P., Konert, M., Kars, S., Peat, H., Smith, R.I.L., Convey, P., 2001b. (Poly)phenolic compounds in pollen and spores of Antarctic plants as indicators of UV-B: a new proxy for the reconstruction of past solar UV-B? Plant Ecol. 154, 11–26.

Rozema, J., Blokker, P., Mayoral Fuertes, M.A., Broekman, R., 2009. UV-B absorbing compounds in present-day and fossil pollen, spores, cuticles, seed coats and wood: evaluation of a proxy for solar UV radiation. Photochem. Photobiol. Sci. 8, 1233–1243.

Rubenstein, C.V., Gerriene, P., de la Puente, G.S., Astini, R.A., Steemans, P., 2010. Early Middle Ordovician evidence for land plants in Argentina (eastern Gondwana). New Phytol. 188, 365–369.

Schulte, F., Lingott, J., Panne, U., Kneipp, J., 2008. Chemical characterization and classification of pollen. Anal. Chem. 80, 9551–9556.

Schulte, F., Panne, U., Kneipp, J., 2010. Molecular changes during pollen germination can be monitored by Raman microspectroscopy. J. Biophotonics 3, 542–547.

Traverse, A., 2007. Paleopalynology. second ed. Springer, Dordrecht.

Watson, J.S., Septhon, M.A., Sephton, S.V., Self, S., Fraser, W.T., Lomax, B.H., Gilmour, I., Wellman, C.H., Beerling, D.J., 2007. Rapid determination of spore chemistry using thermochemolysis gas chromatography–mass spectrometry and micro-Fourier transform infrared spectroscopy. Photochem. Photobiol. Sci. 6, 689–694.

Watson, J.S., Fraser, W.T., Sephton, M.A., 2012. Formation of a polyalkyl macromolecule from the hydrolysable component within sporopollenin during heating/pyrolysis experiments with Lycopodium spores. J. Anal. Appl. Pyrolysis 95, 138–144.

Willis, K.J., Feurdean, A., Birks, H.J.B., Bjune, A.E., Breman, E., Broekman, R., Grytnes, J.A., New, M., Singarayer, J.S., Rozema, J., 2011. Quantification of UV-B flux through time using UV-B-absorbing compounds contained in fossil Pinus sporopollenin. New Phytol. 192, 553–560.

Zimmermann, B., 2010. Characterization of pollen by vibrational spectroscopy. Appl. Spectrosc. 64, 1364–1373.

Zimmermann, B., Kohler, A., 2014. Infrared spectroscopy of pollen identifies plant species and genus as well as environmental conditions. PLoS One 9, 1–12.

Zimmermann, B., Bagcioglu, M., Sandt, C., Kohler, A., 2015a. Vibrational microspectroscopy enables chemical characterization of single pollen grains as well as comparative analysis of plant species based on pollen ultrastructure. Planta 242, 1237–1250.

Zimmermann, B., Tkalčec, Z., Mešić, A., Kohler, A., 2015b. Characterizing aeroallergens by infrared spectroscopy of fungal spores and pollen. PLoS One 10, 1–22.